

# Static Analysis of Functionally Graded Plates Using Higher-Order Shear Deformation Theory

B. Sidda Reddy<sup>a\*</sup>, J. Suresh Kumar<sup>b</sup>, C. Eswara Reddy<sup>c</sup>, and K. Vijaya Kumar Reddy<sup>b</sup>

<sup>a</sup> School of Mechanical Engineering, R. G. M. College of Engineering and Technology, Nandyal, Kurnool (Dt), Andhra Pradesh, India

<sup>b</sup> Department of Mechanical Engineering, J. N. T. U. H. College of Engineering, J. N. T. University, Hyderabad, India

<sup>c</sup> School of Engineering & Technology, Sri Padmavathi Mahila Visvavidyalayam, Women's University, Tirupati, Chittoor, Andhra Pradesh, India

**Abstract:** This paper presents analytical formulations and solutions for the static analysis of functionally graded plates (FGPs) using higher order shear deformation theory (HSDT) without enforcing zero transverse shear stress on the top and bottom surfaces of the plate. The theoretical model presented herein incorporates the transverse extensibility which accounts for the transverse effects. The equations of equilibrium and boundary conditions are derived using the principle of virtual work. Solutions are obtained for FGPs in closed-form using Navier's technique. The results are compared with the other HSDTs for deflections and stresses. It can be concluded that the proposed theory is accurate and efficient in predicting the static responses of functionally graded plates. The results show that, the effect of transverse shear deformation is quite significant at side-to-thickness ratio less than 10 on maximum center deflections and stresses and the response of FGPs is intermediate to that of ceramic and metal plates.

**Keywords:** Static analysis; functionally graded plates; HSDT; Navier's method.

## 1. Introduction

Functionally graded materials (FGMs) are a new generation of engineered materials in which the material properties are continually varied through the thickness direction by mixing two different materials and thus no distinct internal boundaries exist and failures from interfacial stress concentrations developed in conventional structural components can be avoided. FGMs are widely used in many structural applications such as mechanics, civil engineering, optical, electronic, chemical, mechanical, biomedical, energy sources, nuclear, automotive fields and ship building industries to eliminate stress concentration and relax residual stresses and enhance bond strength.

The literature on the FGPs is relatively scarce when compared to isotropic and laminated plates. Because of FGMs applications in high temperature environments, most of the studies on the behavior of FGM plates focus on the thermo-mechanical response of FGM plates: Reddy and chin [1], Reddy [2], Vel and Batra [3, 4], Cheng and Batra [5] and Javaheri and Eslami [6]. In the past, a variety of plate theories have been proposed to study the mechanical behavior of FGM

---

\* Corresponding author; e-mail: [sidhareddy548@gmail.com](mailto:sidhareddy548@gmail.com)

Received 18 April 2013

Revised 10 October 2013

Accepted 30 October 2013

plates. In particular, knowledge pertaining to static analysis is essential for optimal design of structures. For example, our numerical results clearly show that, one could achieve an optimal design for FGM plates with a suitable power law index “ $n$ ”.

The Classical plate theory (CPT) provides acceptable results only for the analysis of thin plates and neglects the transverse shear effects. However, for moderately thick plates CPT under predicts deflections and over predicts buckling loads and natural frequencies. The first-order shear deformation theories (FSDTs) are based on Reissner [7] and Mindlin [8] accounts for the transverse shear deformation effect by means of a linear variation of in-plane displacements and stresses through the thickness of the plate, but requires a correction factor to satisfy the free transverse shear stress conditions on the top and bottom surfaces of the plate. Although, the FSDT provides a sufficiently accurate description of response for thin to moderately thick plates, it is not convenient to use due to difficulty with determination of the correct value of shear correction factor [9]. In-order to overcome the limitations of FSDT many HSDTs were developed that involve higher order terms in Taylor's expansions of the displacements in the thickness coordinate, notable among them are Reddy [2], Zenkour [10-12], Kant and Co-workers [13-18], Kadkhodayan [19], Matsunaga [20, 21], Xiang [22] and Ferreira [23]. Most of these theories do not account for transverse shear stress on the top and bottom surfaces of the plate and transverse extensibility by neglecting the transverse stress in the  $z$ -direction ( $\sigma_z$ ). Mechab et.al [25] developed a two variable refined plate theory to the bending analysis of functionally graded plates; Mantari and Soares [26] used the new trigonometric higher order shear deformation theory with stretching effect to develop the analytical solutions for static analysis of functionally graded materials. They employed the virtual work principle to derive the governing equations of motion and boundary conditions. The bi-sinusoidal load in the transverse direction is applied to the simply supported FGM plate to obtain the Navier-type solution. Vo and Thai [9] developed a new sinusoidal shear deformation theory based on the assumption that the in-plane and transverse displacements consist of bending and shear parts to predict the bending, buckling and vibration responses of FGM plates. The material properties are graded according to a power law distribution of the volume fraction of the constituents. They used Hamilton's principle to derive the equations of motion. Neves et.al [23, 24] derived a higher order shear deformation theory (HSDT) for modeling of functionally graded material plates and focused on the thickness stretching issue on the static, free vibration, and buckling analysis of FGM plates by a meshless technique. They used the virtual work principle of displacements under Carrera's Unified Formulation (CUF) to obtain the governing equations and boundary conditions. The bending and Eigen problems are solved by collocation with radial basis functions.

The present paper deals with the analytical formulations and solutions for the static analysis of functionally graded plates (FGPs) using higher order shear deformation theory (HSDT) without enforcing zero transverse shear stress on the top and bottom surfaces of the plate. The theoretical model presented herein incorporates the transverse extensibility which accounts for the transverse effects. Thus a shear correction factor is not required. The plate material is graded through the thickness direction. The plate's governing equations and its boundary conditions are derived by employing the principle of virtual work. Navier-type analytical solution is obtained for plates subjected to transverse sinusoidal load for simply supported boundary conditions. The results are compared with other higher order shear deformation theories available in the literature to verify the accuracy of the proposed theory in predicting the static responses of FG plates. To make the study feasible, the displacements and stresses are given for different homogenization schemes and exponents in the power law that describes through the thickness variation of the constituents.

## 2. Theoretical formulation

In formulating the higher-order shear deformation theory, a rectangular plate of length  $a$ , width  $b$  and thickness  $h$  is considered, that composed of functionally graded material through the thickness. Figure 1 shows the functionally graded material plate with the rectangular Cartesian coordinate system  $x$ ,  $y$  and  $z$ . The material properties are assumed to be varied in the thickness direction only and the bright and dark areas correspond to ceramic and metal particles respectively. On the top surface ( $z=+h/2$ ), the plate is composed of full ceramic and graded to the bottom surface ( $z=-h/2$ ) that composed of full metal. The reference surface is the middle surface of the plate ( $z=0$ ). The functionally graded material plate properties are assumed to be the function of the volume fraction of constituent materials. The functional relationship between the material property and the thickness coordinates is assumed to be

$$P(z) = (P_t - P_b) \left( \frac{z}{h} + \frac{1}{2} \right)^n + P_b \quad (1)$$

where  $P$  denoted's the effective material property,  $P_t$  and  $P_b$  denotes the property on the top and bottom surface of the plate respectively and  $n$  is the material variation parameter that dictates the material variation profile through the thickness. The effective material properties of the plate, including Young's modulus,  $E$ , density  $\rho$ , and shear modulus,  $G$ , vary according to Equation (1), and poisons ratio ( $\nu$ ) is assumed to be constant.

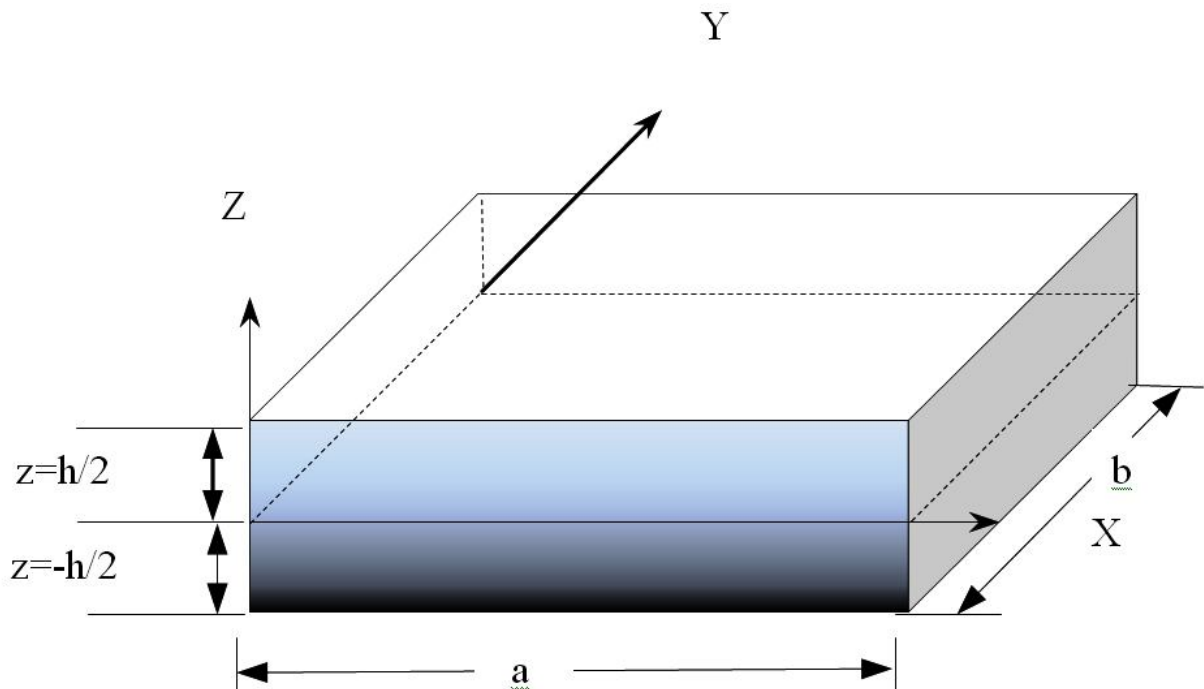


Figure 1. Functionally graded plate and coordinates

### 2.1. Displacement models

In order to approximate 3D plate problem to a 2D one, the displacement components  $u(x, y, z, t)$ ,  $v(x, y, z, t)$  and  $w(x, y, z, t)$  at any point in the plate are expanded in terms of the thickness

coordinate. The elasticity solution indicates that the transverse shear stress varies parabolically through the plate thickness. This requires the use of a displacement field, in which the in-plane displacements are expanded as cubic functions of the thickness coordinate. In addition, the transverse normal strain may vary nonlinearly through the plate thickness. The displacement field which satisfies the above criteria may be assumed in the form [27]:

$$\left. \begin{aligned} u(x, y, z) &= u_0(x, y) + z\theta_x(x, y) + z^2 u_0^*(x, y) + z^3 \theta_x^*(x, y) \\ v(x, y, z) &= v_0(x, y) + z\theta_y(x, y) + z^2 v_0^*(x, y) + z^3 \theta_y^*(x, y) \\ w(x, y, z) &= w_0(x, y) + z\theta_z(x, y) + z^2 w_0^*(x, y) + z^3 \theta_z^*(x, y) \end{aligned} \right\} \quad (2)$$

where

$u_0, v_0$  is the in plane displacements of a point  $(x, y)$  on the mid plane.

$w_0$  is the transverse displacement of a point  $(x, y)$  on the mid plane.

$\theta_x, \theta_y, \theta_z$  are rotations of the normal to the mid plane about  $y$  and  $x$ -axes.

$u_0^*, v_0^*, w_0^*, \theta_x^*, \theta_y^*$ , and  $\theta_z^*$  are the corresponding higher order deformation terms.

By substitution of displacement relations from Equation (2) into the strain displacement equations of the classical theory of elasticity the following relations are obtained:

$$\varepsilon_x = \varepsilon_{x0} + zk_x + z^2 \varepsilon_{x0}^* + z^3 k_x^* \quad (3a)$$

$$\varepsilon_y = \varepsilon_{y0} + zk_y + z^2 \varepsilon_{y0}^* + z^3 k_y^* \quad (3b)$$

$$\varepsilon_z = \varepsilon_{z0} + zk_z + z^2 \varepsilon_{z0}^* \quad (3c)$$

$$\gamma_{xy} = \varepsilon_{xy0} + zk_{xy} + z^2 \varepsilon_{xy0}^* + z^3 k_{xy}^* \quad (3d)$$

$$\gamma_{yz} = \phi_y + zK_{yz} + z^2 \phi_y^* + z^3 k_{yz}^* \quad (3e)$$

$$\gamma_{xz} = \phi_x + zK_{xz} + z^2 \phi_x^* + z^3 k_{xz}^* \quad (3f)$$

where

$$\varepsilon_{x0} = \frac{\partial u_0}{\partial x}, \quad \varepsilon_{y0} = \frac{\partial v_0}{\partial y}, \quad \varepsilon_{xy0} = \frac{\partial u_0}{\partial y} + \frac{\partial v_0}{\partial x}$$

$$\varepsilon_{z0} = \theta_z, \quad k_z = 2w_0^*$$

$$k_x = \frac{\partial \theta_x}{\partial x}, \quad k_y = \frac{\partial \theta_y}{\partial y}, \quad k_{xy} = \frac{\partial \theta_x}{\partial y} + \frac{\partial \theta_y}{\partial x}$$

$$k_x^* = \frac{\partial \theta_x^*}{\partial x}, \quad k_y^* = \frac{\partial \theta_y^*}{\partial y},$$

$$k_{xy}^* = \frac{\partial \theta_x^*}{\partial y} + \frac{\partial \theta_y^*}{\partial x}$$

$$\varepsilon_{x0}^* = \frac{\partial u_0^*}{\partial x}, \quad \varepsilon_{y0}^* = \frac{\partial v_0^*}{\partial y}, \quad \varepsilon_{xy0}^* = \frac{\partial u_0^*}{\partial y} + \frac{\partial v_0^*}{\partial x},$$

$$\begin{aligned}\varepsilon_{z0}^* &= 3\theta_z^*, \phi_y = \theta_y + \frac{\partial w_0}{\partial y}, \phi_x = \theta_x + \frac{\partial w_0}{\partial x}, \\ \phi_x^* &= 3\theta_x^* + \frac{\partial w_0^*}{\partial x}, k_{xz}^* = \frac{\partial \theta_z^*}{\partial x}, k_{xz} = 2u_0^* + \frac{\partial \theta_z}{\partial x}, \\ \phi_y^* &= 3\theta_y^* + \frac{\partial w_0^*}{\partial y}, k_{yz}^* = \frac{\partial \theta_z^*}{\partial y}, k_{yz} = 2v_0^* + \frac{\partial \theta_z}{\partial y}\end{aligned}$$

## 2.2. Elastic stress-strain relations

The elastic stress-strain relations depend on which assumption of  $\varepsilon_z$  we consider. If  $\varepsilon_z \neq 0$ , i.e., thickness stretching is allowed then the 3D model is used. In the case of functionally graded materials the constitutive equations can be written as:

$$\begin{Bmatrix} \sigma_x \\ \sigma_y \\ \sigma_z \\ \tau_{xy} \\ \tau_{yz} \\ \tau_{xz} \end{Bmatrix} = \begin{bmatrix} Q_{11} & Q_{12} & Q_{13} & 0 & 0 & 0 \\ Q_{12} & Q_{22} & Q_{23} & 0 & 0 & 0 \\ Q_{13} & Q_{23} & Q_{33} & 0 & 0 & 0 \\ 0 & 0 & 0 & Q_{44} & 0 & 0 \\ 0 & 0 & 0 & 0 & Q_{55} & 0 \\ 0 & 0 & 0 & 0 & 0 & Q_{66} \end{bmatrix} \begin{Bmatrix} \varepsilon_x \\ \varepsilon_y \\ \varepsilon_z \\ \gamma_{xy} \\ \gamma_{yz} \\ \gamma_{xz} \end{Bmatrix} \quad (4)$$

Where ( $\sigma_x, \sigma_y, \sigma_z, \tau_{xy}, \tau_{yz}, \tau_{xz}$ ) are the stresses and ( $\varepsilon_x, \varepsilon_y, \varepsilon_z, \gamma_{xy}, \gamma_{yz}, \gamma_{xz}$ ) are the strains with respect to the axes,  $Q_{ij}$ 's are the plane stress reduced elastic coefficients in the plate axes that vary through the plate thickness given by

$$\begin{aligned}Q_{11} = Q_{22} = Q_{33} &= \frac{(1-\nu^2)E(z)}{1-3\nu^2-2\nu^3}; & Q_{12} = Q_{13} = Q_{23} &= \frac{\nu(1+\nu)E(z)}{1-3\nu^2-2\nu^3}, \\ Q_{44} = Q_{55} = Q_{66} &= \frac{E(z)}{2(1+\nu)}; & E(z) &= (E_c - E_m) \left( \frac{z}{h} + \frac{1}{2} \right)^n + E_m\end{aligned} \quad (5)$$

where  $E_c$  is the modulus of Elasticity of the ceramic material and  $E_m$  is the modulus of elasticity of the metal.

## 2.3. Governing equations of motion

The governing equations of motion of present theory are derived using the Hamilton's principle can be written in the analytical form as:

$$\int_0^T (\delta U + \delta V - \delta K) dt = 0 \quad (6)$$

Where  $\delta U$  is the virtual strain energy,  $\delta V$  is the virtual work done by applied forces, and  $\delta K$  is the virtual kinetic energy and is given by:

$$\delta U = \int_A \left\{ \int_{-h/2}^{h/2} [\sigma_x \delta \epsilon_x + \sigma_y \delta \epsilon_y + \sigma_z \delta \epsilon_z + \tau_{xy} \delta \gamma_{xy} + \tau_{xz} \delta \gamma_{xz} + \tau_{yz} \delta \gamma_{yz}] dz \right\} dx dy \quad (7)$$

$$\delta V = - \int q \delta w^+ dx dy \quad (8)$$

where  $w^+ = w_0 + \frac{h}{2} \theta_z + \frac{h^2}{4} w_0^* + \frac{h^3}{8} \theta_z^*$  is the transverse displacement of any point on the top surface of the plate and q is the transverse load applied at the top surface of the plate.

$$\begin{aligned} \delta K = \int_A \left\{ \int_{-h/2}^{h/2} \rho_0 \left[ (\dot{u}_0 + Z \dot{\theta}_x + Z^2 \dot{u}_0^* + Z^3 \dot{\theta}_x^*) (\delta \dot{u}_0 + Z \delta \dot{\theta}_x + Z^2 \delta \dot{u}_0^* + Z^3 \delta \dot{\theta}_x^*) \right. \right. \\ \left. \left. + (\dot{v}_0 + Z \dot{\theta}_y + Z^2 \dot{v}_0^* + Z^3 \dot{\theta}_y^*) (\delta \dot{v}_0 + Z \delta \dot{\theta}_y + Z^2 \delta \dot{v}_0^* + Z^3 \delta \dot{\theta}_y^*) \right. \right. \\ \left. \left. + (\dot{w}_0 + Z \dot{\theta}_z + Z^2 \dot{w}_0^* + Z^3 \dot{\theta}_z^*) (\delta \dot{w}_0 + Z \delta \dot{\theta}_z + Z^2 \delta \dot{w}_0^* + Z^3 \delta \dot{\theta}_z^*) \right] dz \right\} dx dy \quad (9) \end{aligned}$$

Substituting for  $\delta U$ ,  $\delta V$  and  $\delta K$  in the virtual work statement in Equation (6) and integrating through the thickness, integrating by parts and collecting the coefficients of  $\delta u_0, \delta v_0, \delta w_0, \delta \theta_x, \delta \theta_y, \delta \theta_z, \delta u_0^*, \delta v_0^*, \delta w_0^*, \delta \theta_x^*, \delta \theta_y^*, \delta \theta_z^*$  the following equations of motion are obtained.

$$\delta u_0 : \frac{\partial N_x}{\partial x} + \frac{\partial N_{xy}}{\partial y} = I_1 \ddot{u}_0 + I_2 (\ddot{\theta}_x) + I_3 \ddot{u}_0^* + I_4 \ddot{\theta}_x^* \quad (10a)$$

$$\delta v_0 : \frac{\partial N_y}{\partial y} + \frac{\partial N_{xy}}{\partial x} = I_1 \ddot{v}_0 + I_2 (\ddot{\theta}_y) + I_3 \ddot{v}_0^* + I_4 \ddot{\theta}_y^* \quad (10b)$$

$$\delta w_0 : \frac{\partial Q_x}{\partial x} + \frac{\partial Q_y}{\partial y} + q = I_1 \ddot{w}_0 + I_2 \ddot{\theta}_z + I_3 \ddot{w}_0^* + I_4 \ddot{\theta}_z^* \quad (10c)$$

$$\delta \theta_x : \frac{\partial M_x}{\partial x} + \frac{\partial M_{xy}}{\partial y} - Q_x = I_2 \ddot{u}_0 + I_3 (\ddot{\theta}_x) + I_4 \ddot{u}_0^* + I_5 \ddot{\theta}_x^* \quad (10d)$$

$$\delta \theta_y : \frac{\partial M_y}{\partial y} + \frac{\partial M_{xy}}{\partial x} - Q_y = I_2 \ddot{v}_0 + I_3 (\ddot{\theta}_y) + I_4 \ddot{v}_0^* + I_5 \ddot{\theta}_y^* \quad (10e)$$

$$\delta \theta_z : \frac{\partial S_x}{\partial x} + \frac{\partial S_y}{\partial y} - N_z + \frac{h}{2} (q) = I_2 \ddot{w}_0 + I_3 \ddot{\theta}_z + I_4 \ddot{w}_0^* + I_5 \ddot{\theta}_z^* \quad (10f)$$

$$\delta u_0^* : \frac{\partial N_x^*}{\partial x} + \frac{\partial N_{xy}^*}{\partial y} - 2S_x = I_3 \ddot{u}_0 + I_4 (\ddot{\theta}_x) + I_5 \ddot{u}_0^* + I_6 \ddot{\theta}_x^* \quad (10g)$$

$$\delta v_0^* : \frac{\partial N_y^*}{\partial y} + \frac{\partial N_{xy}^*}{\partial x} - 2S_y = I_3 \ddot{v}_0 + I_4 (\ddot{\theta}_y) + I_5 \ddot{v}_0^* + I_6 \ddot{\theta}_y^* \quad (10h)$$

$$\delta w_0^* : \frac{\partial Q_x^*}{\partial x} + \frac{\partial Q_y^*}{\partial y} - 2M_z + \frac{h^2}{4} (q) = I_3 \ddot{w}_0 + I_4 \ddot{\theta}_z + I_5 \ddot{w}_0^* + I_6 \ddot{\theta}_z^* \quad (10i)$$

$$\delta\theta_x^* : \frac{\partial M_x^*}{\partial x} + \frac{\partial M_{xy}^*}{\partial y} - 3Q_x^* = I_4 \ddot{u}_0 + I_5 (\ddot{\theta}_x) + I_6 \ddot{u}_0^* + I_7 \ddot{\theta}_x^* \quad (10j)$$

$$\delta\theta_y^* : \frac{\partial M_y^*}{\partial y} + \frac{\partial M_{xy}^*}{\partial x} - 3Q_y^* = I_4 \ddot{v}_0 + I_5 (\ddot{\theta}_y) + I_6 \ddot{v}_0^* + I_7 \ddot{\theta}_y^* \quad (10k)$$

$$\delta\theta_z^* : \frac{\partial S_x}{\partial x} + \frac{\partial S_y}{\partial y} - 3N_z^* + \frac{h^3}{8} (q) = I_4 \ddot{w}_0 + I_5 \ddot{\theta}_z + I_6 \ddot{w}_0^* + I_7 \ddot{\theta}_z^* \quad (10l)$$

Where the in-plane force and moment resultants are defined as:

$$\begin{Bmatrix} N_x & | & N_x^* \\ N_y & | & N_y^* \\ N_z & | & N_z^* \\ N_{xy} & | & N_{xy}^* \end{Bmatrix} = \sum_{L=1}^n \int_{-h/2}^{h/2} \begin{Bmatrix} \sigma_x \\ \sigma_y \\ \sigma_z \\ \tau_{xy} \end{Bmatrix} [I | z^2] dz \quad (11)$$

$$\begin{Bmatrix} M_x & | & M_x^* \\ M_y & | & M_y^* \\ M_z & | & 0 \\ M_{xy} & | & M_{xy}^* \end{Bmatrix} = \sum_{L=1}^n \int_{-h/2}^{h/2} \begin{Bmatrix} \sigma_x \\ \sigma_y \\ \sigma_z \\ \tau_{xy} \end{Bmatrix} [Z | Z^3] dz \quad (12)$$

and the transverse force resultants and inertias are given by:

$$\begin{Bmatrix} Q_x & | & Q_x^* \\ Q_y & | & Q_y^* \end{Bmatrix} = \sum_{L=1}^n \int_{-h/2}^{h/2} \begin{Bmatrix} \tau_{xz} \\ \tau_{yz} \end{Bmatrix} [I | Z^2] dz \quad (13)$$

$$\begin{Bmatrix} S_x & | & S_x^* \\ S_y & | & S_y^* \end{Bmatrix} = \sum_{L=1}^n \int_{-h/2}^{h/2} \begin{Bmatrix} \tau_{xz} \\ \tau_{yz} \end{Bmatrix} [Z | Z^3] dz \quad (14)$$

$$I_1, I_2, I_3, I_4, I_5, I_6, I_7 = \int_{-h/2}^{h/2} \rho_0 (1, Z, Z^2, Z^3, Z^4, Z^5, Z^6) dz \quad (15)$$

The resultants in Equations (11)-(14) can be related to the total strains in Equation (4) by the following matrix:

$$\begin{Bmatrix} N \\ N^* \\ \dots \\ M \\ M^* \\ \dots \\ Q \\ Q^* \end{Bmatrix} = \begin{bmatrix} A & | & B & | & 0 \\ B^t & | & D_b & | & \bar{0} \\ \bar{0} & | & \bar{0} & | & D_s \end{bmatrix} \begin{Bmatrix} \epsilon_0 \\ \epsilon_0^* \\ \dots \\ K_s \\ K^* \\ \dots \\ \phi \\ \phi^* \end{Bmatrix} \quad (16)$$

where

$$N = [N_x \ N_y \ N_z \ N_{xy}]^t ; N^* = [N_x^* \ N_y^* \ N_z^* \ N_{xy}^*]^t$$

$$M = [M_x \ M_y \ M_z \ M_{xy}]^t ; M^* = [M_x^* \ M_y^* \ M_z^* \ M_{xy}^*]^t$$

$$Q = [Q_x \ Q_y \ S_x \ S_y]^t ; Q^* = [Q_x^* \ Q_y^* \ S_x^* \ S_y^*]^t$$

$$\varepsilon_0 = [\varepsilon_{x0} \ \varepsilon_{y0} \ \varepsilon_{z0} \ \varepsilon_{xy0}]^t ; \varepsilon_0^* = [\varepsilon_{x0}^* \ \varepsilon_{y0}^* \ \varepsilon_{z0}^* \ \varepsilon_{xy0}^*]^t$$

$$K = [K_x \ K_y \ K_z \ K_{xy}]^t ; K^* = [K_x^* \ K_y^* \ 0 \ K_{xy}^*]^t$$

$$\phi = [\phi_x \ \phi_y \ k_{xz} \ k_{yz}]^t ; \phi^* = [\phi_x^* \ \phi_y^* \ k_{xz}^* \ K_{yz}^*]^t$$

The matrices [A], [B], [D] and [Ds] are the plate stiffness whose elements can be calculated using Equation (4), and Equations (11)-(14).

### 3. Analytical solutions

Rectangular plates are generally classified by referring to the type of support used. We are here concerned with the analytical solutions of the Equations (10)-(16) for simply supported FG plates. Exact solutions of the partial differential Equation (10) an arbitrary domain and for general boundary conditions are difficult. Although, the Navier-type solutions can be used to validate the present higher order theory, more general boundary conditions will require solution strategies involving, e.g., boundary discontinuous double Fourier series approach.

Solution functions that completely satisfy the boundary conditions in Equations (17) are assumed as follows:

$$u_0(x, y) = \sum_{m=1}^{\infty} \sum_{n=1}^{\infty} U_{mn} \cos \alpha x \sin \beta y, \quad 0 \leq x \leq a; \quad 0 \leq y \leq b; \quad (17a)$$

$$v_0(x, y, t) = \sum_{m=1}^{\infty} \sum_{n=1}^{\infty} V_{mn} \sin \alpha x \cos \beta y, \quad 0 \leq x \leq a; \quad 0 \leq y \leq b; \quad (17b)$$

$$w_0(x, y) = \sum_{m=1}^{\infty} \sum_{n=1}^{\infty} W_{mn} \sin \alpha x \sin \beta y, \quad 0 \leq x \leq a; \quad 0 \leq y \leq b; \quad (17c)$$

$$\theta_x(x, y) = \sum_{m=1}^{\infty} \sum_{n=1}^{\infty} X_{mn} \cos \alpha x \sin \beta y, \quad 0 \leq x \leq a; \quad 0 \leq y \leq b; \quad (17d)$$

$$\theta_y(x, y) = \sum_{m=1}^{\infty} \sum_{n=1}^{\infty} Y_{mn} \sin \alpha x \cos \beta y, \quad 0 \leq x \leq a; \quad 0 \leq y \leq b; \quad (17e)$$

$$\theta_z(x, y) = \sum_{m=1}^{\infty} \sum_{n=1}^{\infty} Z_{mn} \sin \alpha x \sin \beta y, \quad 0 \leq x \leq a; \quad 0 \leq y \leq b; \quad (17f)$$

$$u_0^*(x, y) = \sum_{m=1}^{\infty} \sum_{n=1}^{\infty} U_{mn}^* \cos \alpha x \sin \beta y, \quad 0 \leq x \leq a; \quad 0 \leq y \leq b; \quad (17g)$$

$$v_o^*(x, y) = \sum_{m=1}^{\infty} \sum_{n=1}^{\infty} V_{mn}^* \sin \alpha x \cos \beta y, \quad 0 \leq x \leq a; \quad 0 \leq y \leq b; \quad (17h)$$

$$w_o^*(x, y) = \sum_{m=1}^{\infty} \sum_{n=1}^{\infty} W_{mn}^* \sin \alpha x \sin \beta y, \quad 0 \leq x \leq a; \quad 0 \leq y \leq b; \quad (17i)$$

$$\theta_x^*(x, y) = \sum_{m=1}^{\infty} \sum_{n=1}^{\infty} X_{mn}^* \cos \alpha x \sin \beta y, \quad 0 \leq x \leq a; \quad 0 \leq y \leq b; \quad (17j)$$

$$\theta_y^*(x, y) = \sum_{m=1}^{\infty} \sum_{n=1}^{\infty} Y_{mn}^* \sin \alpha x \cos \beta y, \quad 0 \leq x \leq a; \quad 0 \leq y \leq b; \quad (17k)$$

$$\theta_z^*(x, y) = \sum_{m=1}^{\infty} \sum_{n=1}^{\infty} Z_{mn}^* \sin \alpha x \sin \beta y, \quad 0 \leq x \leq a; \quad 0 \leq y \leq b; \quad (17l)$$

where  $\alpha = \frac{m\pi}{a}$  and  $\beta = \frac{n\pi}{b}$  and m and n are modes numbers.

And the mechanical load is expanded in double Fourier sine series as:

$$q(x, y) = \sum_{m=1}^{\infty} \sum_{n=1}^{\infty} Q_{mn} \sin \alpha x \sin \beta y \quad (18)$$

Substituting Equations (17a)-(17l) in to Equation (10) and collecting the coefficients one obtains

$$[S]_{12 \times 12} \begin{Bmatrix} U_{mn} \\ V_{mn} \\ W_{mn} \\ X_{mn} \\ Y_{mn} \\ Z_{mn} \\ U_{mn}^* \\ V_{mn}^* \\ W_{mn}^* \\ X_{mn}^* \\ Y_{mn}^* \\ Z_{mn}^* \end{Bmatrix} = \begin{Bmatrix} 0 \\ 0 \\ Q_{mn} \\ 0 \\ 0 \\ \frac{h}{2} Q_{mn} \\ 0 \\ 0 \\ \frac{h^2}{4} Q_{mn} \\ 0 \\ 0 \\ \frac{h^3}{8} Q_{mn} \end{Bmatrix} \quad (19)$$

For any fixed value of m and n. The elements of the coefficient matrix [S] are as follows.

Solutions of the Equation (19) are obtained for each m, n=1, 2, ... as  $U_{mn}, V_{mn}, W_{mn}, X_{mn}, Y_{mn}, Z_{mn}, U_{mn}^*, V_{mn}^*, W_{mn}^*, X_{mn}^*, Y_{mn}^*, Z_{mn}^*$ , which are used to compute  $u_o, v_o, w_o, \theta_x, \theta_y, \theta_z, u_o^*, v_o^*, w_o^*, \theta_x^*, \theta_y^*, \theta_z^*$ .

$$\begin{aligned}
 S_{1,1} &= A_{1,1}\alpha^2 + A_{4,4}\beta^2 & S_{1,2} &= (A_{1,2} + A_{4,4})\alpha\beta & S_{1,3} &= 0 \\
 S_{1,4} &= B_{1,1}\alpha^2 + B_{4,4}\beta^2 & S_{1,5} &= (B_{1,2} + B_{4,4})\alpha\beta & S_{1,6} &= -A_{1,3}\alpha \\
 S_{1,7} &= A_{1,5}\alpha^2 + A_{4,8}\beta^2 & S_{1,8} &= (A_{4,8} + A_{1,6})\alpha\beta & S_{1,9} &= -2B_{1,3}\alpha \\
 S_{1,10} &= B_{1,5}\alpha^2 + B_{4,8}\beta^2 & S_{1,11} &= (B_{1,6} + B_{4,8})\alpha\beta & S_{1,12} &= -3A_{1,7} \\
 \\
 S_{2,1} &= (A_{2,1} + A_{4,4})\alpha\beta & S_{2,2} &= A_{4,4}\alpha^2 + A_{2,2}\beta^2 & S_{2,3} &= 0 \\
 S_{2,4} &= (B_{2,1} + B_{4,4})\alpha\beta & S_{2,5} &= B_{4,4}\alpha^2 + B_{2,2}\beta^2 & S_{2,6} &= -A_{2,3}\beta \\
 S_{2,7} &= (A_{4,8} + A_{2,5})\alpha\beta & S_{2,8} &= A_{4,8}\alpha^2 + A_{2,6}\beta^2 & S_{2,9} &= -2B_{2,3}\beta \\
 S_{2,10} &= (B_{2,5} + B_{4,8})\alpha\beta & S_{2,11} &= B_{4,8}\alpha^2 + B_{2,6}\beta^2 & S_{2,12} &= -3A_{2,7}\beta \\
 \\
 S_{3,1} &= 0 & S_{3,2} &= 0 & S_{3,3} &= D_{1,1}^s\alpha^2 + D_{2,2}^s\beta^2 \\
 S_{3,4} &= D_{1,1}^s\alpha & S_{3,5} &= D_{2,2}^s\beta & S_{3,6} &= D_{1,3}^s\alpha^2 + D_{2,4}^s\beta^2 \\
 S_{3,7} &= 2D_{1,3}^s\alpha & S_{3,8} &= 2D_{2,4}^s\beta & S_{3,9} &= D_{1,5}^s\alpha^2 + D_{2,6}^s\beta^2 \\
 S_{3,10} &= 3D_{1,5}^s\alpha & S_{3,11} &= 3D_{2,6}^s\beta & S_{2,12} &= D_{1,7}^s\alpha^2 + D_{2,8}^s\beta^2 \\
 \\
 S_{4,1} &= B_{1,1}\alpha^2 + B_{4,4}\beta^2 & S_{4,2} &= (B_{2,1} + B_{4,4})\alpha\beta & S_{4,3} &= D_{1,1}^s\alpha \\
 S_{4,4} &= D_{1,1}\alpha^2 + D_{4,4}\beta^2 + D_{1,1}^s & S_{4,5} &= (D_{1,2} + D_{4,4})\alpha\beta & S_{4,6} &= (D_{1,3}^s - B_{3,1})\alpha \\
 S_{4,7} &= B_{5,1}\alpha^2 + B_{8,4}\beta^2 + 2D_{1,3}^s & S_{4,8} &= (B_{6,1} + B_{8,4})\alpha\beta & S_{4,9} &= (D_{1,5}^s - 2D_{1,3})\alpha \\
 S_{4,10} &= D_{1,5}\alpha^2 + D_{4,8}\beta^2 + 3D_{1,5}^s & S_{4,11} &= (D_{1,6} + D_{4,8})\alpha\beta & S_{4,12} &= (D_{1,7}^s - 3B_{7,1})\alpha \\
 \\
 S_{5,1} &= (B_{1,2} + B_{4,4})\alpha\beta & S_{5,2} &= B_{4,4}\alpha^2 + B_{2,2}\beta^2 & S_{5,3} &= D_{2,2}^s\beta \\
 S_{5,4} &= (D_{2,1} + D_{4,4})\alpha\beta & S_{5,5} &= D_{4,4}\alpha^2 + D_{2,2}\beta^2 + D_{2,2}^s & S_{5,6} &= (D_{2,4}^s - B_{3,2})\beta \\
 S_{5,7} &= (B_{5,2} + B_{8,4})\alpha\beta & S_{5,8} &= B_{8,4}\alpha^2 + B_{6,2}\beta^2 + 2D_{2,4}^s & S_{5,9} &= (D_{2,6}^s - 2D_{2,3})\beta \\
 S_{5,10} &= (D_{2,5} + D_{4,8})\alpha\beta & S_{5,11} &= D_{4,8}\alpha^2 + D_{2,6}\beta^2 + 3D_{2,6}^s & S_{5,12} &= (D_{2,8}^s - 3B_{7,2})\beta \\
 \\
 S_{6,1} &= -A_{3,1}\alpha & S_{6,2} &= -A_{3,2}\beta & S_{6,3} &= D_{3,1}^s\alpha^2 + D_{4,2}^s\beta^2 \\
 S_{6,4} &= D_{3,1}^s\alpha - B_{3,1}\alpha & S_{6,5} &= (D_{4,2}^s - B_{3,2})\beta & S_{6,6} &= D_{3,3}^s\alpha^2 + D_{4,4}^s\beta^2 + A_{3,3} \\
 S_{6,7} &= (2D_{3,3}^s - A_{3,5})\alpha & S_{6,8} &= (2D_{4,4}^s - A_{3,6})\beta & S_{6,9} &= D_{3,5}^s\alpha^2 + D_{4,6}^s\beta^2 + 2B_{3,3} \\
 S_{6,10} &= (3D_{3,5}^s - B_{3,5})\alpha & S_{6,11} &= (3D_{4,6}^s - B_{3,6})\beta & S_{6,12} &= D_{3,7}^s\alpha^2 + D_{4,8}\beta^2 + 3A_{3,7} \\
 \\
 S_{7,1} &= A_{5,1}\alpha^2 + A_{8,4}\beta^2 & S_{7,2} &= (A_{5,2} + A_{8,4})\alpha\beta & S_{7,3} &= 2D_{3,1}^s\alpha \\
 S_{7,4} &= B_{5,1}\alpha^2 + B_{8,4}\beta^2 + 2D_{3,1}^s & S_{7,5} &= (B_{5,2} + B_{8,4})\alpha\beta & S_{7,6} &= (2D_{3,3}^s - A_{5,3})\alpha \\
 S_{7,7} &= A_{5,5}\alpha^2 + A_{8,8}\beta^2 + 4D_{3,3}^s & S_{7,8} &= (A_{5,6} + A_{8,8})\alpha\beta & S_{7,9} &= (2D_{3,5}^s - 2B_{5,3})\alpha \\
 S_{7,10} &= B_{5,5}\alpha^2 + B_{8,8}\beta^2 + 6D_{3,5}^s & S_{7,11} &= (B_{5,6} + B_{8,8})\alpha\beta & S_{7,12} &= (2D_{3,7}^s - 3A_{5,7})\alpha \\
 \\
 S_{8,1} &= (A_{6,1} + A_{8,4})\alpha\beta & S_{8,2} &= A_{8,4}\alpha^2 + A_{6,2}\beta^2 & S_{8,3} &= 2D_{4,2}^s\beta \\
 S_{8,4} &= (B_{6,1} + B_{8,4})\alpha\beta & S_{8,5} &= B_{8,4}\alpha^2 + B_{6,2}\beta^2 + 2D_{4,2}^s & S_{8,6} &= (2D_{4,4}^s - A_{6,3})\beta \\
 S_{8,7} &= (A_{6,5} + A_{8,8})\alpha\beta & S_{8,8} &= A_{8,8}\alpha^2 + A_{6,6}\beta^2 + 4D_{4,4}^s & S_{8,9} &= (2D_{4,6}^s - 2B_{6,3})\beta \\
 S_{8,10} &= (B_{6,5} + B_{8,8})\alpha\beta & S_{8,11} &= B_{8,8}\alpha^2 + B_{6,6}\beta^2 + 6D_{4,6}^s & S_{8,12} &= (2D_{4,8}^s - 3A_{6,7})\beta
 \end{aligned}$$

$$\begin{aligned}
 S_{9,1} &= -2B_{1,3}\alpha & S_{9,2} &= -2B_{2,3}\beta & S_{9,3} &= D_{5,1}^S \alpha^2 + D_{6,2}^S \beta^2 \\
 S_{9,4} &= (D_{5,1}^S - 2D_{3,1})\alpha & S_{9,5} &= (D_{6,2}^S - 2D_{3,2})\beta & S_{9,6} &= D_{5,3}^S \alpha^2 + D_{6,4}^S \beta^2 + 2B_{3,3} \\
 S_{9,7} &= (2D_{5,3}^S - 2B_{5,3})\alpha & S_{9,8} &= (2D_{6,4}^S - 2B_{6,3})\beta & S_{9,9} &= D_{5,5}^S \alpha^2 + D_{6,6}^S \beta^2 + 4D_{3,3} \\
 S_{9,10} &= (3D_{5,5}^S - 2D_{3,5})\alpha & S_{9,11} &= (3D_{6,6}^S - 2D_{3,6})\beta & S_{9,12} &= D_{5,7}^S \alpha^2 + D_{6,8}^S \beta^2 + 6B_{7,3} \\
 S_{10,1} &= B_{1,5}\alpha^2 + B_{4,8}\beta^2 & S_{10,2} &= (B_{2,5} + B_{4,8})\alpha\beta & S_{10,3} &= 3D_{5,1}^S \alpha \\
 S_{10,4} &= D_{5,1}^S \alpha^2 + D_{8,4}\beta^2 + 3D_{5,1}^S & S_{10,5} &= (D_{5,2} + D_{8,4})\alpha\beta & S_{10,6} &= (3D_{5,3}^S - B_{3,5})\alpha \\
 S_{10,7} &= B_{5,5}\alpha^2 + B_{8,8}\beta^2 + 6D_{5,3}^S & S_{10,8} &= (B_{6,5} + B_{8,8})\alpha\beta & S_{10,9} &= (3D_{5,5}^S - 2D_{5,3})\alpha \\
 S_{10,10} &= D_{5,5}^S \alpha^2 + D_{8,8}\beta^2 + 9D_{5,5}^S & S_{10,11} &= (D_{5,6} + D_{8,8})\alpha\beta & S_{10,12} &= (D_{5,7}^S - 3B_{7,5})\alpha \\
 S_{11,1} &= (B_{1,6} + B_{4,8})\alpha\beta & S_{11,2} &= B_{4,8}\alpha^2 + B_{2,6}\beta^2 & S_{11,3} &= 3D_{6,2}^S \beta \\
 S_{11,4} &= (D_{6,1} + D_{8,4})\alpha\beta & S_{11,5} &= D_{8,4}\alpha^2 + D_{6,2}\beta^2 + 3D_{6,2}^S & S_{11,6} &= (3D_{6,4}^S - B_{3,6})\beta \\
 S_{11,7} &= (B_{5,6} + B_{8,8})\alpha\beta & S_{11,8} &= B_{8,8}\alpha^2 + B_{6,6}\beta^2 + 6D_{6,4}^S & S_{11,9} &= (3D_{6,6}^S - 2D_{6,3})\beta \\
 S_{11,10} &= (D_{6,5} + D_{8,8})\alpha\beta & S_{11,11} &= D_{8,8}\alpha^2 + D_{6,6}\beta^2 + 9D_{6,6}^S & S_{11,12} &= (3D_{6,8}^S - 3B_{7,6})\beta \\
 S_{12,1} &= -3A_{7,1}\alpha & S_{12,2} &= -3A_{7,2}\beta & S_{12,3} &= D_{7,1}^S \alpha^2 + D_{8,2}^S \beta^2 \\
 S_{12,4} &= (D_{7,1}^S - 3B_{7,1})\alpha & S_{12,5} &= (D_{8,2}^S - 3B_{7,2})\beta & S_{12,6} &= D_{7,3}^S \alpha^2 + D_{8,4}^S \beta^2 + 3A_{7,3} \\
 S_{12,7} &= (2D_{7,3}^S - 3A_{7,5})\alpha & S_{12,8} &= (2D_{8,4}^S - 3A_{7,6})\beta & S_{12,9} &= D_{7,5}^S \alpha^2 + D_{8,6}^S \beta^2 + 6B_{7,3} \\
 S_{12,10} &= (3D_{7,5}^S - 3B_{7,5})\alpha & S_{12,11} &= (3D_{8,6}^S - 3B_{7,6})\beta & S_{12,12} &= D_{7,7}^S \alpha^2 + D_{8,8}^S \beta^2 + 9A_{7,7}
 \end{aligned}$$

#### 4. Results and discussion

In this section, a numerical example is presented and discussed to verify the accuracy of the present higher-order shear deformation theory in predicting the deflections and stresses of a simply supported functionally graded material plate. For numerical results, an Al/Al<sub>2</sub>O<sub>3</sub> Plate is considered and graded from aluminum (as metal) at the bottom to alumina (as ceramic) at the top surface of the plate. The material properties adopted here are Aluminium Young's modulus ( $E_m$ ): 70GPa , density  $\rho_m= 2702 \text{ kg/m}^3$ , and Poisson's ratio ( $\nu$ ): 0.3 Alumina Young's modulus ( $E_c$ ): 380GPa, density  $\rho_c= 3800\text{kg/m}^3$ , and Poisson's ratio ( $\nu$ ): 0.3.

For convenience, the transverse displacement, in-plane and the transverse shear stresses are presented in nondimensionalized form as

$$\begin{aligned}
 \bar{w} &= 10w_0 \left( \frac{a}{2}, \frac{b}{2} \right) \times \frac{E_c h^3}{qa^4}; \quad \bar{\sigma}_x = \frac{h}{aq} \sigma_x \left( \frac{a}{2}, \frac{b}{2}, \frac{h}{2} \right); \quad \bar{\sigma}_y = \frac{h}{aq} \sigma_y \left( \frac{a}{2}, \frac{b}{2}, \frac{h}{3} \right); \\
 \bar{\tau}_{xy} &= \frac{h}{aq} \tau_{xy} \left( 0, 0, -\frac{h}{3} \right); \quad \bar{\tau}_{yz} = \frac{h}{aq} \tau_{yz} \left( \frac{a}{2}, 0, \frac{h}{6} \right); \quad \bar{\tau}_{xz} = \frac{h}{aq} \tau_{xz} \left( 0, \frac{b}{2}, 0 \right) \quad \text{and} \quad \bar{z} = \frac{z}{h}
 \end{aligned}$$

In Table 1 we present results for normal stresses and transverse displacements for various material variation parameters “ $n$ ” of the power law. The considered side-to-thickness ratios ( $a/h$ ) are 4, 10 and 100. Results are compared with the Carrera et al. [28, 29] and Neves et al. [24, 30].

The results from present higher-order shear deformation theory considering  $\epsilon z \neq 0$  are in good agreement with those from Refs. [24, 28, 29 and 30] who also considers  $\epsilon z \neq 0$ . It can also be seen that the effect of the exponent “ $n$ ” of the power law on the dimensionless deflections and stresses

of an FGM plate is being demonstrated in the results presented in Table 1. As the exponent value “n” increases, the difference increases for deflection and decreases for in-plane longitudinal stress ( $\bar{\sigma}_x$ ) and also for a/h decreases. The maximum percentage error observed between present higher order shear deformation theory and Neves et al. is 17.86 for normal stress ( $\bar{\sigma}_x$ ) at side-to-thickness ratio 4 and power law index 10. Results in Table 1 should serve as benchmark results for future comparisons.

**Table 1.** Comparison of nondimensional normal stress  $\bar{\sigma}_x$  and center deflections(w)

| n   | Theory         | $\bar{\sigma}_x (h/3)$ |                 |                  | $\bar{w}$       |                 |                 |
|-----|----------------|------------------------|-----------------|------------------|-----------------|-----------------|-----------------|
|     |                | a/h                    |                 |                  | a/h             |                 |                 |
|     |                | 4                      | 10              | 100              | 4               | 10              | 100             |
| 0   | Ref.[24]       | 0.527800               | 1.317600        | 13.161000        | 0.366500        | 0.294200        | 0.280300        |
|     | <b>Present</b> | <b>0.548990</b>        | <b>1.325320</b> | <b>13.172600</b> | <b>0.366501</b> | <b>0.294254</b> | <b>0.280403</b> |
| 0.5 | Ref.[24]       | 0.586000               | 1.468000        | 14.673000        | 0.549300        | 0.454800        | 0.436500        |
|     | <b>Present</b> | <b>0.611335</b>        | <b>1.474280</b> | <b>14.646100</b> | <b>0.553451</b> | <b>0.452037</b> | <b>0.432540</b> |
| 1   | Ref.[29]       | 0.622100               | 1.506400        | 14.969000        | 0.717100        | 0.587500        | 0.562500        |
|     | Ref.[28]       | 0.622100               | 1.506400        | 14.969000        | 0.717100        | 0.587500        | 0.562500        |
|     | Ref.[30]       | 0.592500               | 1.494500        | 14.969000        | 0.699700        | 0.584500        | 0.562400        |
|     | Ref.[24]       | 0.591100               | 1.491700        | 14.945000        | 0.702000        | 0.586800        | 0.564700        |
|     | <b>Present</b> | <b>0.627707</b>        | <b>1.508120</b> | <b>14.969400</b> | <b>0.717416</b> | <b>0.587536</b> | <b>0.562532</b> |
| 4   | Ref.[29]       | 0.487700               | 1.197100        | 11.923000        | 1.158500        | 0.882100        | 0.828600        |
|     | Ref.[28]       | 0.487700               | 1.197100        | 11.923000        | 1.158500        | 0.882100        | 0.828600        |
|     | Ref.[30]       | 0.440400               | 1.178300        | 11.932000        | 1.117800        | 0.875000        | 0.828600        |
|     | Ref.[24]       | 0.433000               | 1.158800        | 11.737000        | 1.110800        | 0.870000        | 0.824000        |
|     | <b>Present</b> | <b>0.507926</b>        | <b>1.204310</b> | <b>11.9234</b>   | <b>1.157040</b> | <b>0.881670</b> | <b>0.828682</b> |
| 10  | Ref.[29]       | 0.369500               | 0.896500        | 8.907700         | 1.374500        | 1.007200        | 0.936100        |
|     | Ref.[28]       | 0.147800               | 0.896500        | 8.907700         | 1.374500        | 1.007200        | 0.936100        |
|     | Ref.[30]       | 0.322700               | 1.178300        | 11.932000        | 1.349000        | 0.875000        | 0.828600        |
|     | Ref.[24]       | 0.309700               | 0.846200        | 8.601000         | 1.333400        | 0.988800        | 0.922700        |
|     | <b>Present</b> | <b>0.377067</b>        | <b>0.887084</b> | <b>8.908000</b>  | <b>1.376930</b> | <b>1.007180</b> | <b>0.936184</b> |

Figures 2-3 show the variation of maximum centre deflection against side-to-thickness ratios (a/h) and aspect ratios (a/b) for various power law exponents “n”. From Figures 2-3, it is observed that the deflections are larger for metal rich plates and decreases as the plate becomes more and more ceramic. This is due to the fact that the Young’s modulus of ceramic ( $E_c=380\text{GPa}$ ) is higher than that of the metal ( $E_m=70\text{GPa}$ ). Hence for FGM plates, the transverse deflection is intermediate to that of metal and ceramic rich plates. In addition, the difference in deflection of the FGM plates decreases as the aspect ratio increases, while it may be unchanged with the increase of side-to-thickness ratio. The effect of transverse shear deformation is felt at side-to-thickness ratio less than 10. Also, as aspect ratio (a/b) increases the maximum center deflections decreases. This is due to the increase of stiffness of the plate.

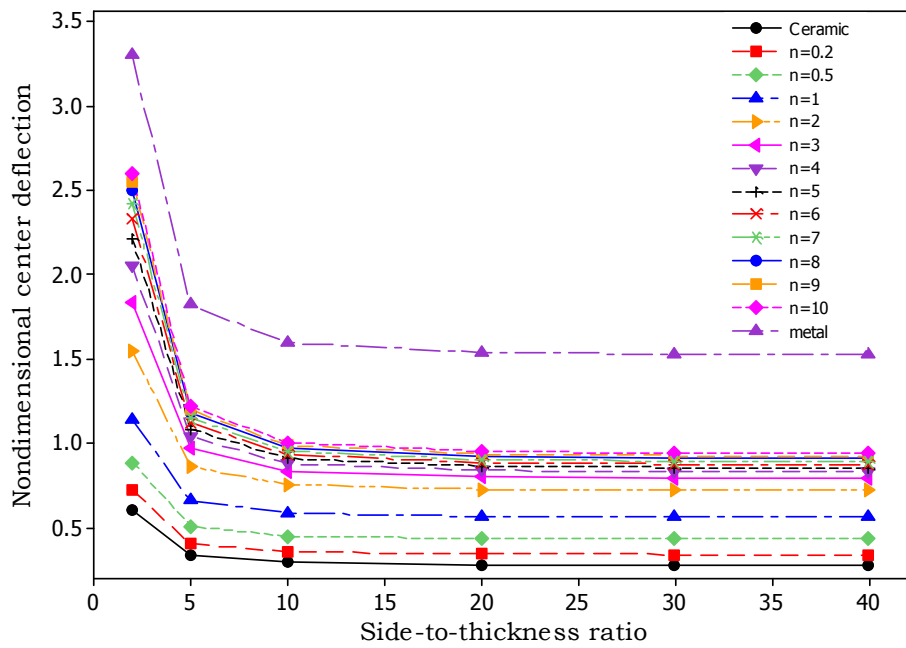


**Figure 2.** Nondimensional displacement ( $\bar{w}$ ) as a function of side-to-thickness ratio ( $a/h$ ) of an FGM plate for various values of power law index ( $n$ )

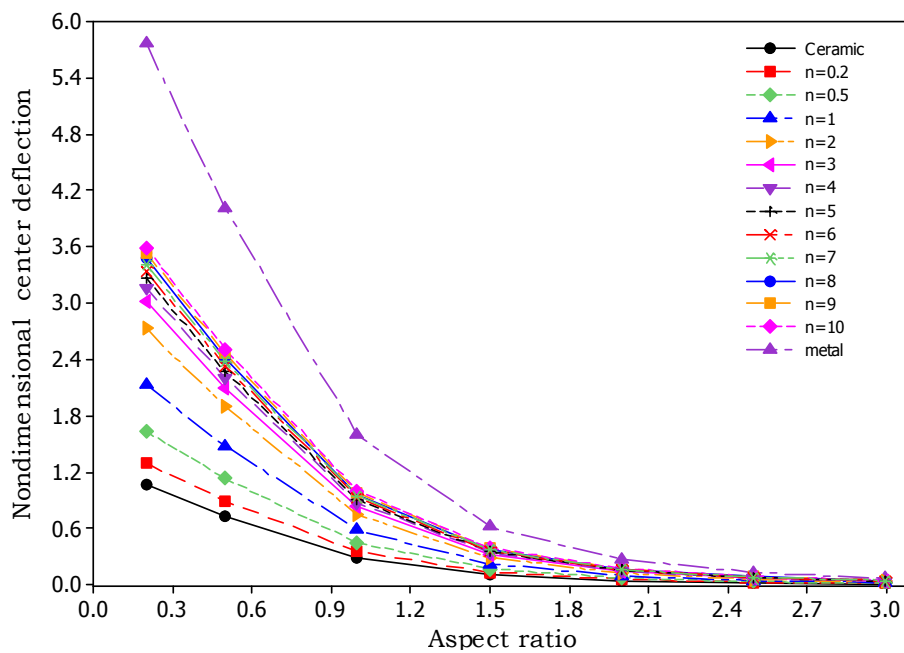


**Figure 3.** Nondimensional displacement ( $\bar{w}$ ) as a function of Aspect ratio ( $a/b$ ) of an FGM plate for various values of power law index ( $n$ )

Figures 4-5 show the variation of nondimensionalized maximum normal stressses ( $\bar{\sigma}_x$  and  $\bar{\sigma}_y$ ) against aspect ratio for FGM square plate as a function of power law index. From Figure 4, it is observed that the nondimensionalized maximum normal stress ( $\sigma_x$ ) decreases with the increase of aspect ratio and decrease of power law index. This is due to the increase of stiffness of the plate. But normal stress increases with aspect ratio up to 0.5 and then decreases

gradually. It is due to the increase of elastic constants  $Q_{ij}$ .

The variation of nondimensionalized normal stress  $\bar{\sigma}_z$  against modulus ratio as a function of power law index is shown in Figure 6. From the Figure 6 it is seen that, the nondimensionalized normal stress  $\bar{\sigma}_z$  increases with increase of modulus ratio and power law index. The reason is as the mixture of metal-ceramic ratio increases, the metal-ceramic modulli increases. Hence normal stress  $\bar{\sigma}_z$  increases.

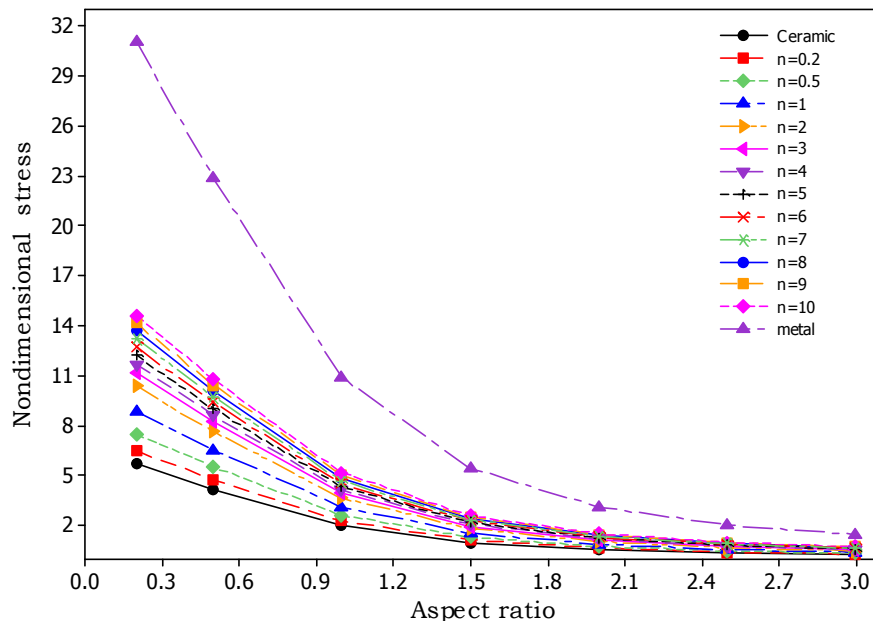


**Figure 4.** Nondimensional stress ( $\bar{\sigma}_x$ ) as a function of Aspect ratio ( $a/b$ ) of an FGM plate for various values of power law index ( $n$ )

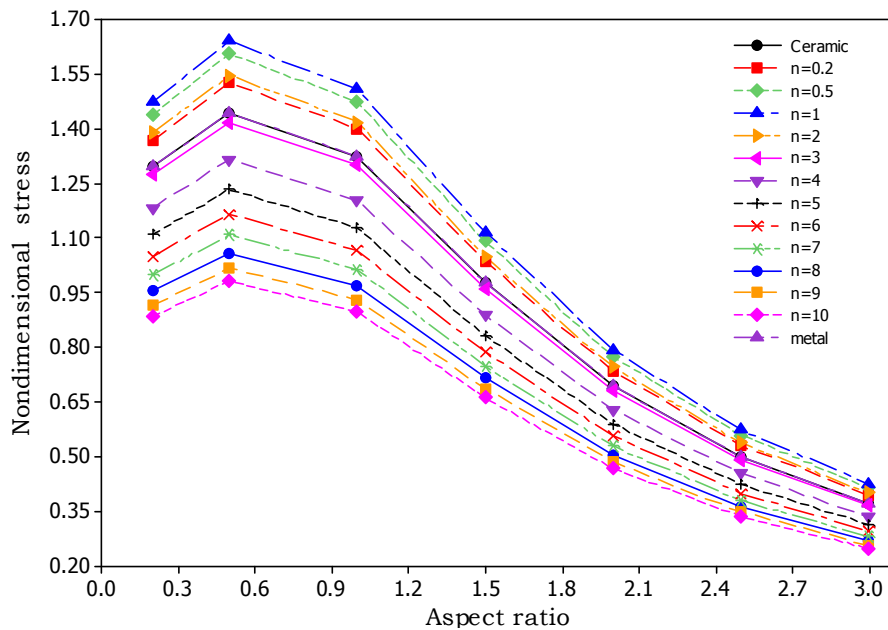


**Figure 5.** Nondimensional stress ( $\bar{\sigma}_y$ ) as a function of Aspect ratio ( $a/b$ ) of an FGM plate for various values of power law index ( $n$ )

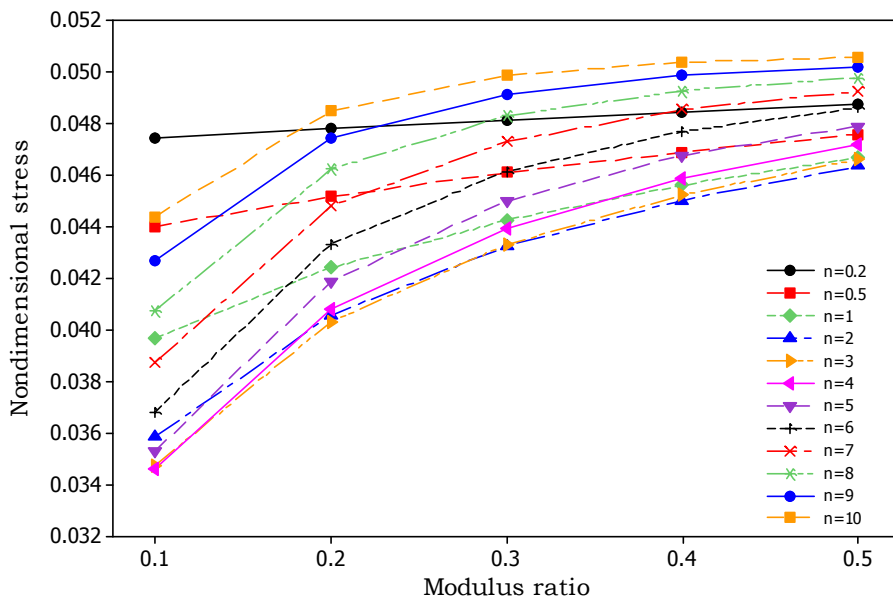


**Figure 6.** Nondimensional stress ( $\bar{\sigma}_z$ ) as a function of Modulus ratio ( $E_m/E_c$ ) of an FGM plate for various values of power law index ( $n$ )

The effect of transverse shear deformation on the nondimensionalized shear stresses ( $\bar{\tau}_{yz}$   $\bar{\tau}_{xz}$ ) is shown in Figures 7-8. From Figures 7 and 8, it is observed that, the shear stresses ( $\bar{\tau}_{yz}$   $\bar{\tau}_{xz}$ ) increases with the increase of side-to-thickness ratio. The shear deformation effect is to decrease the shear stresses and is felt at side-to-thickness ratio less than 10 and diminishes with the increase of side-to-thickness ratio.

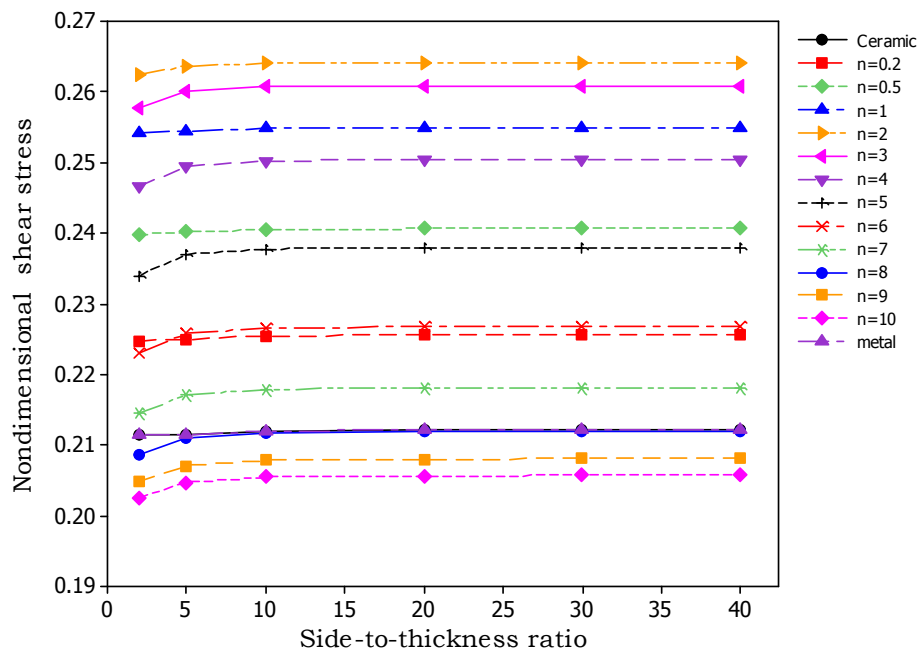


**Figure 7.** Nondimensional shear stress ( $\bar{\tau}_{yz}$ ) as a function of side-to-thickness ratio ( $a/h$ ) of an FGM plate for various values of power law index ( $n$ )

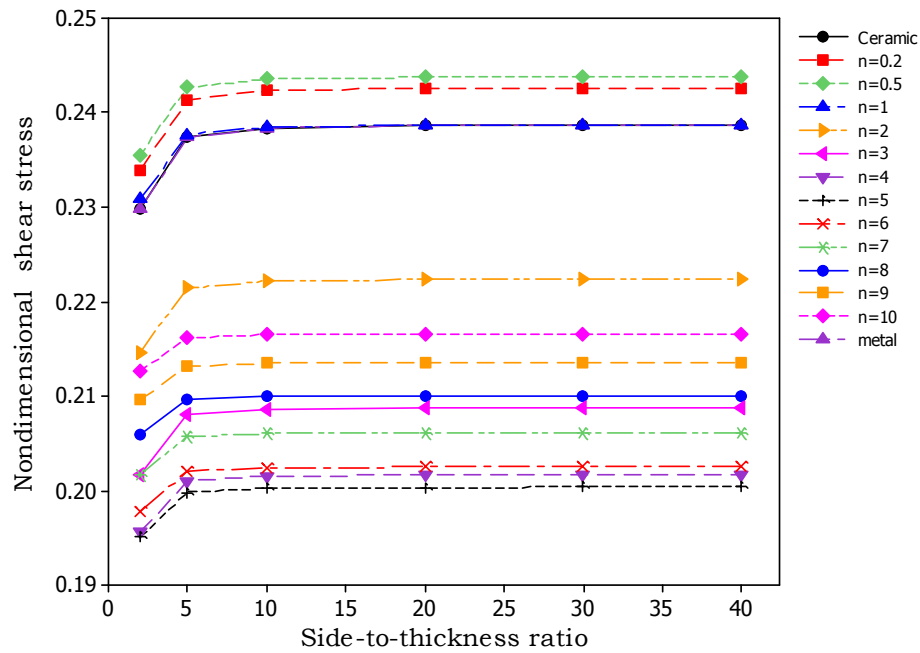


**Figure 8.** Nondimensional shear stress ( $\bar{\tau}_{xz}$ ) as a function of side-to-thickness ratio ( $a/h$ ) of an FGM plate for various values of power law index ( $n$ )

Finally, Figures 9-11 depict the in-plane longitudinal, normal and transverse shear stress distributions across the thickness of the FG plate under the sinusoidal load for different volume fraction exponent of FG plate where side-to-thickness ratio,  $a/h=10$  and aspect ratio,  $a/b=1$ . It can be observed that the stress distribution across the thickness of the plate is not parabolic as in the case of homogeneous plates and the stresses increase as the volume fraction exponent increases. The maximum values of shear stresses  $\bar{\tau}_{xy}$ ,  $\bar{\tau}_{yz}$  and  $\bar{\tau}_{xz}$  occurs at  $\bar{z}=0.2$ , This is due to the non-uniform composition of the material through the plate thickness.

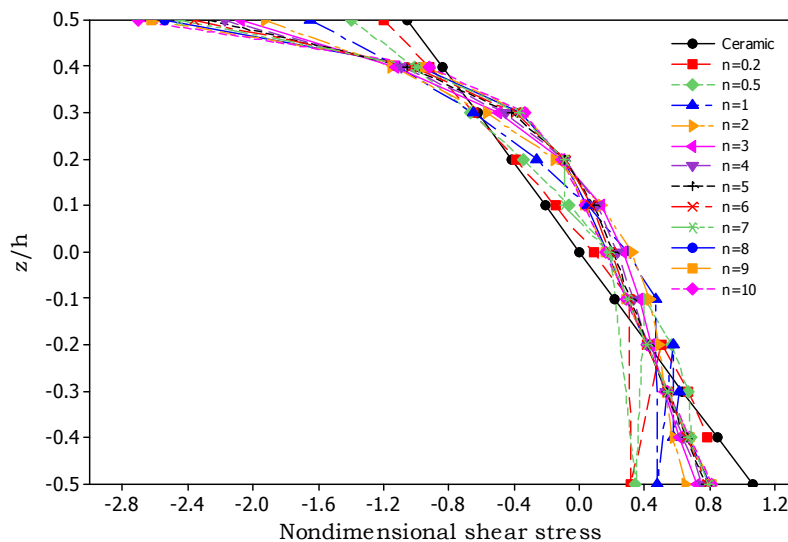


**Figure 9.** Variation of nondimensional shear stress ( $\bar{\tau}_{xy}$ ) across the thickness of an FGM plate for different values of power law index ( $n$ )

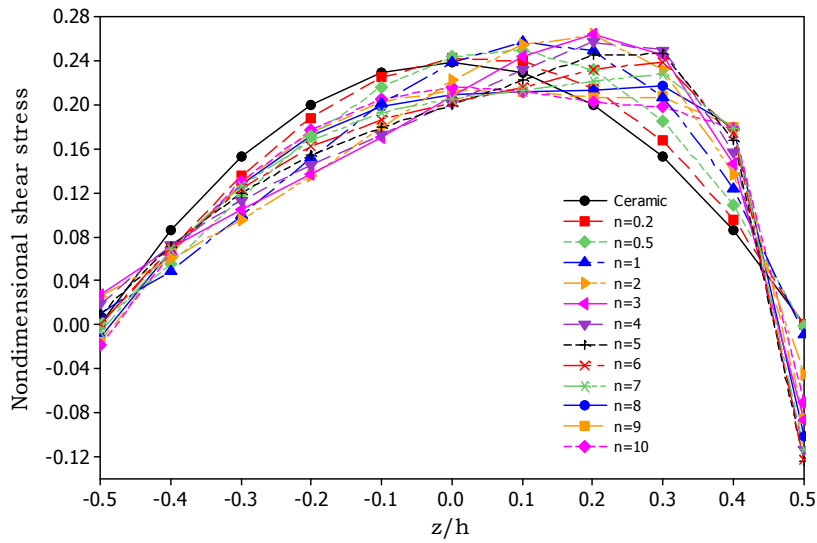


**Figure 10.** Variation of nondimensional shear stress ( $\bar{\tau}_{yz}$ ) across the thickness of an FGM plate for different values of power law index ( $n$ )

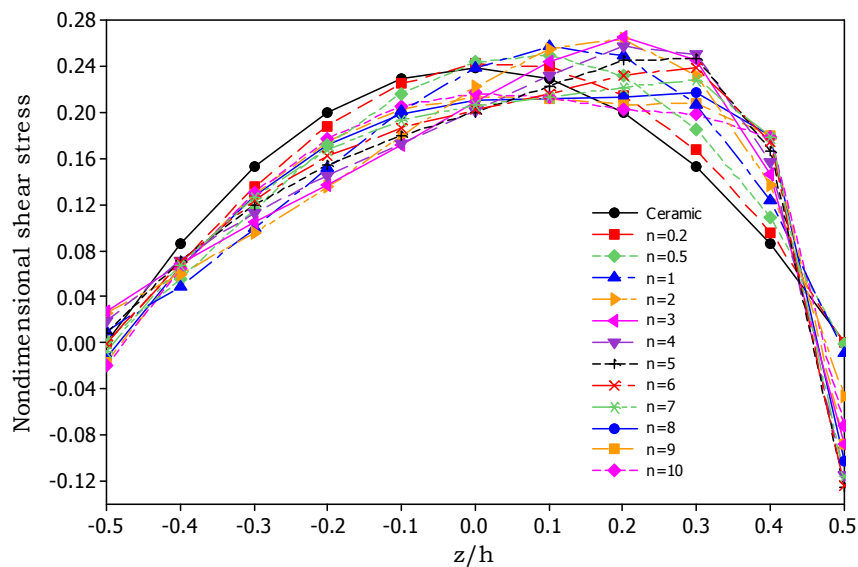


**Figure 11.** Variation of nondimensional shear stress ( $\bar{\tau}_{xz}$ ) across the thickness of an FGM plate for different values of power law index ( $n$ )

## 5. Conclusions

Analytical formulations and solutions for static analysis of functionally graded material plates is developed using a higher-order shear deformation theory considering the  $\epsilon_z$  which account for transverse extensibility and without enforcing zero shear on the top and bottom of the FGM plate. This theory gives parabolic distribution of transverse shear strains. The gradation of properties across the thickness is assumed to be of the power law type. Equations of motion are derived

from the Hamilton's principle. Closed form solutions are obtained for simply supported plates using Naviers method. The accuracy and efficiency of the present theory have been demonstrated in the static behavior of FGM plates. The results are compared with the other higher order shear deformation theory. The results are in good agreement with the Carrera et al. [28, 29] and Neves et al. [24, 30]. In conclusion, it can be said that the gradients in material properties play an important role in static behavior of FG plates and the proposed theory is accurate and simple in analyzing the static behavior of FG plates.

## References

- [ 1] Reddy, J. N. 2000. Analysis of functionally graded plates. *International Journal for Numerical Methods in Engineering*, 47: 663-684.
- [ 2] Reddy, J. N. and Chin, C. D. 1998. Thermomechanical analysis of functionally graded cylinders and plates. *Journal of Thermal Stresses*, 21, 6: 593-626.
- [ 3] Vel, S. S. and Batra, R. C. 2002. Exact solutions for thermoelastic deformations of functionally graded thick rectangular plates. *AIAA Journal*, 40: 1421-1433.
- [ 4] Vel, S. S. and Batra, R. 2003. Three dimensional analysis of transient thermal stresses in functionally graded plates. *International Journal of Solids and Structures*, 40, 25: 7181-7196.
- [ 5] Cheng, Z. Q. and Batra, R. C. 2000. Three dimensional thermoelastic deformations of a functionally graded-elliptic plate. *Composites: Part B*, 31: 97-106.
- [ 6] Javaheri, R. and Eslami, Mr. 2002. Thermal buckling of functionally graded plates based on higher order shear deformation theory. *Journal of Thermal Stresses*, 25, 7: 603-625.
- [ 7] Reissner, E. 1945. The effect of transverse shear deformation on the bending of elastic plates. *Journal of Applied Mechanics: ASME*, 12, 2: 69-77.
- [ 8] Mindlin, R. D. 1951. Influence of rotary inertia and shear on flexural motions of isotropic, elastic plates. *Journal of Applied Mechanics: ASME*, 18: 31-38.
- [ 9] Thai, H. T. and Thuc, P. Vo. 2013. A new sinusoidal shear deformation theory for bending, buckling, and vibration of functionally graded plates. *Applied Mathematical Modelling*, 37: 3269-3281.
- [10] Zenkour, A. M. 2005. A comprehensive analysis of functionally graded sandwich plates: Part-1-Deflection and stresses. *International Journal of Solids and Structures*, 42, 18-19: 5224-5242.
- [11] Zenkour, A. M. 2005. A comprehensive analysis of functionally graded sandwich plates: Part-2-Buckling and free vibration. *International Journal of Solids and Structures*, 42, 18-19: 5243-5258.
- [12] Zenkour, A. M. 2006. Generalized shear deformation theory for bending analysis of functionally graded plates. *Applied Mathematical Modelling*, 30, 1: 67-84.
- [13] Kant, T., Owen, D. R. J., and Zienkiewicz, O. C. 1982. A refined higher order C0 plate element. *Computers & Structures*, 15, 2: 177-183.
- [14] Pandya, B. N. and Kant, T. 1988. Higher-order shear deformable theories for flexure of sandwich plates-finite element evaluations. *International Journal of Solids and Structures*, 24, 12: 1267-1286.
- [15] Pandya, B. N. and Kant, T. 1988. Finite element analysis of laminated composite plates using a higher order displacement model. *Composites Science and Technology*, 32, 2:

- 137-155.
- [16] Kant, T. and Swaminathan, K. 2002. Analytical solutions for the static analysis of laminated composite and sandwich plates based on higher order refined theory. *Composite Structures*, 56, 4: 329-344.
- [17] Kant, T. and Swaminathan, K. 2001. Analytical solutions for free vibration analysis of laminated composite and sandwich plates based on higher order refined theory. *Composite Structures*, 53, 1: 73-85.
- [18] Garg, A. K., Khare, R. K., and Kant, T. 2006. Higher order closed form solutions for free vibration of laminated composite and sandwich shells. *Journal of Sandwich Structures and Materials*, 8, 3: 205-235.
- [19] Golmakani, M. E. and Kadkhodayan, M. 2011. Nonlinear bending analysis of annular FGM plates using higher order shear deformation plate theories. *Composite Structures*, 93: 973-982.
- [20] Matsunaga, H. 2008. Free vibration and stability of functionally graded plates according to a 2-D higher-order deformation theory. *Composite Structures*, 82: 499-512.
- [21] Matsunaga, H. 2009. Stress analysis of functionally graded plates subjected to thermal and mechanical loadings. *Composite Structures*, 87: 344-357.
- [22] Xiang, S. and Kang, G. W. 2013. A nth-order shear deformation theory for the bending analysis on the functionally graded plates. *European Journal of Mechanics-A/Solids*, 37 : 336-343.
- [23] Neves, A. M. A., Ferreira, A. J. M., Carrera, E., Cinefra, M., Roque, C. M. C., Jorge, R. M. N., and Soares, C. M. M. 2013. Free vibration analysis of functionally graded shells by a higher-order shear deformation theory and radial basis functions collocation, accounting for through-the-thickness deformations. *European Journal of Mechanics-A/Solids*, 37: 24-34.
- [24] Neves, A. M. A., Ferreira, A. J. M., Carrera, E., Cinefra, M., Roque, C. M. C., Jorge, R. M. N., and Soares, C. M. M. 2013. Static, free vibration and buckling analysis of isotropic and sandwich functionally graded plates using a quasi-3D higher-order shear deformation theory and meshless technique. *Composites: Part B*, 44: 657-674.
- [25] Mechab, I., Atmane, H. A., Tounsi, A., Belhadej, H. A., and Bedia, E. A. A. 2010. A two variable refined plate theory for the bending analysis of functionally graded plates. *Acta Mechanica Sinica*, 26: 941-949.
- [26] Mantari, J. L. and Guedes Soares, C. 2013. A novel higher-order shear deformation theory with stretching effect for functionally graded plates. *Composites: Part B*, 45: 268-281.
- [27] Kant, T. and Manjunatha, B. S. 1988. An unsymmetric FRC laminate C0 finite element model with 12 degrees of freedom per node. *Engineering with Computers*, 5, 3: 300-308.
- [28] Carrera, E., Brischetto, S., Cinefra, M., and Soave, M. 2011. Effects of thickness stretching in functionally graded plates and shells. *Composites Part B: Engineering*, 42: 123-133.
- [29] Carrera, E., Brischetto, S., and Robaldo, A. 2008. Variable kinematic model for the analysis of functionally graded material plates. *AIAA Journal*, 46: 194-203.
- [30] Neves, A. M. A., Ferreira, A. J. M., Carrera, E., Cinefra, M., Roque, C. M. C., and Jorge, R. M. N. 2012. A quasi-3d sinusoidal shear deformation theory for the static and free vibration analysis of functionally graded plates. *Composites Part B: Engineering*, 43: 711-725.